

Article

# Plant Hydraulic Trait Covariation: A Global Meta-Analysis to Reduce Degrees of Freedom in Trait-Based Hydrologic Models

A. Rio Mursinna <sup>1</sup>, Erica McCormick <sup>1</sup>, Katie Van Horn <sup>2</sup>, Lisa Sartin <sup>3</sup>   
and Ashley M. Matheny <sup>1,\*</sup>

<sup>1</sup> Department of Geological Sciences, University of Texas at Austin, Austin, TX 78712, USA; riogeo@utexas.edu (A.R.M.); erica.mccormick@utexas.edu (E.M.)

<sup>2</sup> Austin Community College, 1218 West Ave. Austin, TX 78701, USA; mkvanhorn@gmail.com

<sup>3</sup> Department of Civil, Environmental, and Geodetic Engineering, Ohio State University, Columbus, OH 43210, USA; sartin.1@osu.edu

\* Correspondence: ashley.matheny@jsg.utexas.edu

Received: 31 May 2018; Accepted: 21 July 2018; Published: 25 July 2018



**Abstract:** Current vegetation modeling strategies use broad categorizations of plants to estimate transpiration and biomass functions. A significant source of model error stems from vegetation categorizations that are mostly taxonomical with no basis in plant hydraulic strategy and response to changing environmental conditions. Here, we compile hydraulic traits from 355 species around the world to determine trait covariations in order to represent hydraulic strategies. Simple and stepwise regression analyses demonstrate the interconnectedness of multiple vegetative hydraulic traits, specifically, traits defining hydraulic conductivity and vulnerability to embolism with wood density and isohydricity. Drought sensitivity is strongly (Adjusted  $R^2 = 0.52$ ,  $p < 0.02$ ) predicted by a stepwise linear model combining rooting depth, wood density, and isohydricity. Drought tolerance increased with increasing wood density and anisohydric response, but with decreasing rooting depth. The unexpected response to rooting depth may be due to other tradeoffs within the hydraulic system. Rooting depth was able to be predicted from sapwood specific conductivity and the water potential at 50% loss of conductivity. Interestingly, the influences of biome or growth form do not increase the accuracy of the drought tolerance model and were able to be omitted. Multiple regression analysis revealed 3D trait spaces and tradeoff axes along which species' hydraulic strategies can be analyzed. These numerical trait spaces can reduce the necessary input to and parameterization of plant hydraulics modules, while increasing the physical representativeness of such simulations.

**Keywords:** hydraulic traits; meta-analysis; hydraulic conductivity; drought tolerance; rooting depth; isohydricity; wood density; plant hydraulics modeling

## 1. Introduction

### 1.1. Functional Trait Covariation

Following Ackerly, et al. [1] plant functional traits ('traits' from here onward) are defined as characteristics of a species or broader group of plants which have significant influence on performance at all stages of life: development, growth, and survival. Traits that have evolved within the lifespan of an individual are considered to be plastic responses to environmental conditions and are known as "plastic traits". Alternatively, innate traits that differentiate species or larger subdivisions of flora are hereditary and are considered to be "adaptive traits" [1]. Adaptations divide plant life into a host of

different resource-use and survival categories. Plants adopt different survival strategies through suites of traits in which define how an individual responds to water, sunlight, nutrients and other stimuli.

The theoretical framework of the plant-economics spectrum has been employed to explain species fitness across light, water, and nutrient gradients, and subsequently the biogeographic distribution of global vegetation [2–6]. For example, in arid climates with sandy soils such as the American Southwest, *Prosopis spp.* (mesquite) allocates resources to vertically extensive root systems in order to access deep water tables. Plants in similar climates nearer to the coast, such as *Baccharis pilularis* DC. (coyote brush, or chaparral broom), are known to make use of the frequent, dense fog that regularly covers the Californian coast through foliar uptake to combat drought conditions. In the context of the plant economics spectrum, significant emphasis is placed on physiology, phenology, and nutrient content (e.g., nitrogen) [7]. In further detail, the leaf-economics spectrum defines the resource allocation as it relates to radiation capture, phylogeny and phenology [6,8]. Facing resource limitations, a plant makes tradeoffs to control fundamental factors regarding carbon assimilation and thus plant growth and survival [9]. Within this tradeoff based framework, Reich, et al. [7] demonstrated that by using climate data, specific leaf area, and plant functional type (PFT), models can reliably predict related traits such as photosynthetic capacity, leaf life span, and nutrient concentrations such as nitrogen and phosphorous. It has also been shown that strong correlations exist among hydraulic traits and plant-carbon economics [10–14]. Zhu, et al. [10] recently showed significant relationships between leaf hydraulic properties (turgor loss point and leaf hydraulic safety margin) with maximum photosynthetic capacity ( $A_{max}$ ) and the water potential at which 50% hydraulic conductivity is lost at the leaf and at the branch. As carbon enters the leaf through stomata, water is lost to transpiration which, in turn, drives water uptake at the roots and through the stem and branches [15], coupling water and carbon use directly.

Similarly to trait-tradeoffs and the “fast” versus “slow” survival strategies of vegetation [4], plant hydraulic traits are likewise hypothesized to trade off along the axis of hydraulic safety versus efficiency [16]. For instance, trees having xylem that are less vulnerable to hydraulic impairment through cavitation, or embolism, tend to be less efficient at water transport than trees with xylem vessels of larger diameter that are often more vulnerable to cavitation [16]. However, in a recent global analysis, Gleason, et al. [17] found only limited support for this direct tradeoff and promoted the roles that additional traits and further tradeoffs may play to complicate this relationship. Understanding strategies of water use and acquisition, often termed hydraulic strategies, and the functional traits that define them is critical to understanding the roles different types and species of vegetation play in the carbon and water cycles, predicting vegetation responses to climate change, and predicting the impacts of drought, disturbances, and other extreme events on the land surface [18]. To that end, Griffin-Nolan, et al. [19] demonstrated that hydraulic traits can be used to predict ecosystem-level responses to changing precipitation patterns. In the context of our changing climate, vegetation regulated feedbacks between the biosphere and atmosphere are expected to change with changing temperature and precipitation [20–24]. Therefore, we narrow our study of plant functional traits to focus specifically on hydraulic functional traits, along with tradeoffs and coordination therein.

## 1.2. Hydraulic Functional Strategies

Vegetation water flux is principally driven by the atmospheric demand for water vapor (VPD) and limited by soil water availability; with all plants striving to maintain sufficient water balance necessary to acquire carbon for survival without succumbing to hydraulic failure [25,26]. Yet, plant species exhibit a broad variety of behaviors in response to atmospheric and soil water-stress limitations within the same ecosystem on the basis of their hydraulic strategy [27–31]. Matheny, et al. [18] identified several potential emergent hydraulic functional traits for the delineation of a species’ integrated ‘whole-plant’ hydraulic strategy including: isohydricity, maximum sapwood conductivity, xylem water potentials at 50% and 88% conductivity loss, and rooting depth. However, this listing is not exhaustive and traits

such as leaf turgor-loss point, hydraulic safety margin, and wood density have also been shown to be integral in predicting drought tolerance [32–38].

Trait correlations have been used to accurately predict physiological processes [7,37,39,40]. In their 2012 study, Choat et al. [37] demonstrated relationships between the xylem water potential at which 50% of conductivity is lost ( $\Psi_{50}$ ), the minimum measured xylem water potential ( $\Psi_{\min}$ ), mean annual precipitation (MAP) and drought vulnerability. Globally, the xylem hydraulic safety margin ( $\Psi_{\min} - \Psi_{50}$ ) of forest tree species was reported as less than 1 MPa for 70% of plants studied [37]. Lower safety margins indicate greater risk of hydraulic failure in the event of drought. Santiago, et al. [40] found that for several canopy trees in the Amazon, xylem efficiency is significantly related to hydraulic capacitance, sapwood water content, and turgor loss point, and thus propose the use of wood density as an easy-to-measure proxy of hydraulic physiology. Correlations may also be likely between rooting depth and drought tolerance within a biome, where deeply-rooted plants can access water at depth and shallowly-rooted plants are therefore less tolerant to drought conditions. For instance, if two shallowly-rooted plants express opposite drought tolerance traits, it could be assumed that the drought tolerator would be anisohydric or having relaxed stomatal response to low leaf water potentials while the drought avoider may maintain rigorous stomatal control and osmoregulation to ensure consistent leaf turgor characteristic of isohydric species [39]. If coordination of plant hydraulic traits exists globally across multiple spatial scales (from organ to individual to biome), as suggested by the work of Choat, et al. [37] and others, special attention should be paid to identifying the coordination and covariations that define tradeoffs within the potential hydraulic trait-space in order to better understand and model the effects of water-stress limitations at large scales, its influence on global biogeography, and its implications for land-atmosphere feedbacks in the context of climate change.

### 1.3. Hydraulic Strategies and the Emergence of Plant Hydrodynamic Models

Plant hydrodynamics models (PHMs) allow for enhanced prediction of vegetation-water use dynamics, and thereby carbon uptake dynamics, of individual plants on the basis of observable hydraulic traits [18,41–43]. Such PHMs are being rapidly adopted into dynamic vegetation and land-surface modeling (LSM) platforms in an effort to improve the simulation of forest function, in terms of carbon and water exchange and their combined influence on expectations of plant growth and mortality [44–46]. With the incorporation of PHMs, one need only know a given species' hydraulic strategy as dictated by fundamental hydraulic traits, to create simulations of vegetation water use and carbon uptake in the presence of given atmospheric and soil conditions [47].

Process-based modeling of water transport through the soil-plant-atmosphere continuum has advanced significantly within the last few years, with the development of new PHMs and their ongoing incorporation into LSMs as replacements for the traditional empirical methods to predict transpiration by calculating stomatal conductance [42,44,45,48]. These models simulate the transport of water in the soil-plant-atmosphere continuum as flow through a porous media, using the Darcy or Richards equations for saturated or unsaturated flow, respectively, and restrict stomatal conductance on the basis of leaf and branch water potentials. Most existing PHMs use a formulation based on Darcy's law which assumes that the transfer of plant-water between the soil and the atmosphere is controlled by vegetation hydraulic conductivity and the hydraulic potential gradient between the soil and the plant [44,49,50]. The most basic class of plant hydraulics models largely ignores factors affecting dynamic changes to xylem capacitance and conductance while focusing instead on total vegetative resistance to water flow [51]. Though this approach has been effective for simulating how drought affects tropical forests at large scales [45], it is incapable of simulating the role of biomass water storage capacity and dynamic changes to capacitance; which have been shown to be equally if not more critical in other ecosystems [41,52]. A more sophisticated set of models tackles this problem by modeling dynamic changes in xylem capacitance as a function of xylem water potential by assuming a relationship between the amount of water stored in the plant and the water potential [42,53].

These PHMs have been shown to significantly improve LSM ability to simulate transpiration and latent heat flux at both the individual plant and the regional scale [44,45,49,54] through realistic prediction of stomatal behavior in response to the dynamics of water availability in the leaf and branch [55,56].

Within these PHM frameworks, observable plant hydraulic traits can be used to define the parameters that govern intra-plant water movement and storage and can greatly improve simulations of transpiration response to water limitations [18]. However, appropriate model parameterization remains a challenge for three principal reasons: (1) the specific hydraulic traits required by PHMs are not uniform across all models; (2) many traits are highly variable, and can be physically difficult to measure leading to a paucity of measurements, particularly within the rhizosphere; and (3) scaling a trait value measured at the leaf or stem-level to the tree, plot, population, and ecosystem levels is complex and nonlinear. As a result, parameter values derived from model optimizations using sap flux or observed ecosystem-level water flux data (frequently from eddy covariance measurements) may not be an exact match for ecological measurement values or be conserved across ecosystems.

The ultimate goal of this work is to identify and explain covariation among plant hydraulic traits in order to reduce the number parameters necessary to create meaningful PHM simulations. This study leverages upon multiple meta-analyses and the resulting databases of compiled vegetation traits from species around the world. We combine hydraulic trait data from multiple datasets in order to establish relationships between the most frequently observed, hydraulically relevant traits in an effort to better constrain physical representations of plant hydraulic behavior on the basis of field-observed traits. Results of work can serve to reduce the required amount of model parameterization to generate PHM simulations for various vegetation types and ecosystems, and provide guidance for observational lists regarding the most critical plant hydraulic traits to monitor in future campaigns. Trait data requirements for PHM simulations can be reduced in cases when statistically meaningful trait covariation exists, i.e., only one (the easier to obtain) of two or more well-correlated values may be necessary for a model to run at comparable accuracy to a model using each trait directly from observations.

#### 1.4. Hypotheses

We hypothesize that hydraulic traits will be significantly coordinated throughout the plant conductive system (i.e., roots, stems, and leaves) in order to form hydraulic strategies. While we hypothesize that biome and growth form (i.e., trees/shrubs/forbs) will be significantly related to many hydraulic traits, we also hypothesize that coordination among traits within species will be stronger than the influence of climate and growth form alone. We further propose that there will exist sufficient trait covariation to allow rooting depth, a challenging trait to measure, to be extrapolated on the basis of more easily observable traits in a manner that will assist in the reduction of degrees of freedom within the trait space required to run many vegetation modeling platforms.

## 2. Methods

Data for this study was compiled from nine studies and databases (Table 1) included within the TRY global plant trait database [57] to generate a global meta-analysis of key vegetation hydraulic traits ( $n = 355$  species). The traits included in this study are biome classification, the unitless shape parameter of xylem vulnerability curve ( $a$ ), conduit density ( $\text{mm}^{-1}$ ), mean annual precipitation (MAP, mm), mean annual temperature (MAT, C),  $\Psi_{50}$  (MPa), drought tolerance (a relative characteristic of a plant's ability to survive in water limited conditions i.e., prolonged periods of dry soil and high vapor pressure deficit which was ranked on a qualitative scale from 0 indicating extremely low drought tolerance to 5 indicating extremely high tolerance), rooting depth (m), sapwood specific conductivity ( $K_{\text{max}}$ ,  $\text{kg m}^{-1} \text{s}^{-1} \text{MPa}^{-1}$ ), growth form (tree, shrub, grass/herb), leaf permanence (a binary variable where 0 indicates deciduousness and 1 indicates evergreen), wood density ( $\text{g cm}^{-3}$ ), and isohydricity ( $\sigma$ , as defined by Martinez-Vilalta, et al. [58]) (Table 1). For species having more than one reported value for a particular trait within the merged database, a species-level mean of that trait was taken.

Species were selected when data were available for six or more of these traits. It is important to note that in the merged database, data for a particular species is brought together from other database and is not necessarily data for one individual in a single location. Biome classifications were only used when more than one species was present to represent each biome. For this reason, boreal, tundra, and taiga ecosystems were not represented within this analysis.

**Table 1.** Variables used in this study and databases from which they were obtained.

Mean Annual Temperature	MAT	Manzoni, et al. [16], Choat, et al. [37], Medlyn, et al. [59]
Mean annual precipitation	MAP	Manzoni, et al. [16], Choat, et al. [37], Medlyn, et al. [59], Preston, et al. [60]
50% loss of hydraulic conductivity	$\Psi_{50}$	Choat, et al. [37], Manzoni, et al. [16]
Slope of cavitation curve at $\Psi_{50}$	$a$	Choat, et al. [37], Manzoni, et al. [16]
Biome	biome	Choat, et al. [37], Martinez-Vilalta, et al. [58]
Rooting depth	$z$	Green [61], Fitter and Peat [62], Diaz, et al. [63]
Drought tolerance	DT	Green [61], Fitter and Peat [62]
Sapwood specific conductivity	$K_{\max}$	Manzoni, et al. [16]
Conduit density	CD	Preston, et al. [60]
Wood density	WD	Chave, et al. [3], Zanne, et al. [64]
Isohydrycity	$\sigma$	Martinez-Vilalta, et al. [58]

All data analysis was conducted using MATLAB (version R2017a, Mathworks, Natick, MA, USA) and assessed through histogram analysis, linear regression and residual analysis, ANOVA and variance testing, boxplot visual analysis, and multiple linear regression analysis with stepwise modeling. Outliers were collected by calculating the average and standard deviation of each set, analyzing histogram distributions to review extreme values, and flagging data further than three standard deviations away from the mean. Furthermore, data for the most xeric species were removed in cases where models became weighted towards outlier trait values. Individual models which appeared to have outlier-driven regressions were subjected to further outlier removal, as noted. Removed outliers are listed in Table S1.

Trait correlation was assessed by taking variables two at a time to generate linear regressions. Equations for fit with  $p$  values below 0.05 and  $R^2$  values above 0.1 were marked as potentially significant. Variables which generated skewed histograms were transformed by taking the logarithm of the dependent variables in order to produce normal distributions. Such instances are noted in the figure captions.

Categorical variables of biome type, leaf permanence, drought, and growth form were used to generate boxplot analysis to visually show deviations in the median between the groups. Boxplots included one continuous variable and two categorical variables for each plot and were used to inform further analyses of variance. While boxplots provide a visual assessment of the difference in medians between the groups, a one-dimensional analysis of variance (ANOVA) was used to determine the variance between the means of groups. Prior to ANOVA tests, data was demonstrated to be normally distributed. The ANOVA returned values of Prob >  $F$  which were interpreted as the likelihood of the given mean variance occurring from random chance. Prob >  $F$  values below 0.05 were considered significant for this study.

Finally, we created multiple linear regression models in order to constrain dependent variables and relate them to the most influential independent variables within our data set. To achieve this, we created tables of three relevant traits and fit multiple linear regression models to them. We assessed the change in  $p$  and  $R^2$  values for linear models as well as models which included various interaction terms. We assessed the models' residuals as histograms, by Cook's distance, by the leverage each observation had on the final model, and by the randomness of the distribution of residuals around the line of fit.

To constrain traits using all of the available variables in this study, we also used a stepwise regression modelling tool. This technique added and removed every trait and possible interaction

term within the specified table and calculated the  $p$  and  $R^2$  for each combination. The best combination of variables was returned as a model. We used this technique for all relevant dependent variables.

### 3. Results

One-dimensional trait relationships were first assessed through regression analysis. Linear regressions were most significant for correlations between  $K_{\max}$  vs. conduit density ( $R^2 = 0.23$ ,  $p = 0.0022$ , Figure S1) and vs.  $\Psi_{50}$  ( $R^2 = 0.19$ ,  $p < 0.0001$ , Figure S3), and the correlation of wood density and  $a$  ( $R^2 = 0.12$ ,  $p < 0.0001$ , Figure S4). The relationship between  $\Psi_{50}$  and isohydricity was significant as well ( $R^2 = 0.19$ ,  $p = 0.005$ , Figure 1), although a regression of root depth and isohydricity was not ( $p = 0.57$ , Figure S7). Isohydric species maintain less negative  $\Psi_{50}$  pressures by reducing stomatal conductance in conditions of excessive VPD (Figure 1).  $P$  values were consistently significant for the majority of relationships, yet  $R^2$  statistics remained low (below 0.3) for most simple linear regressions.

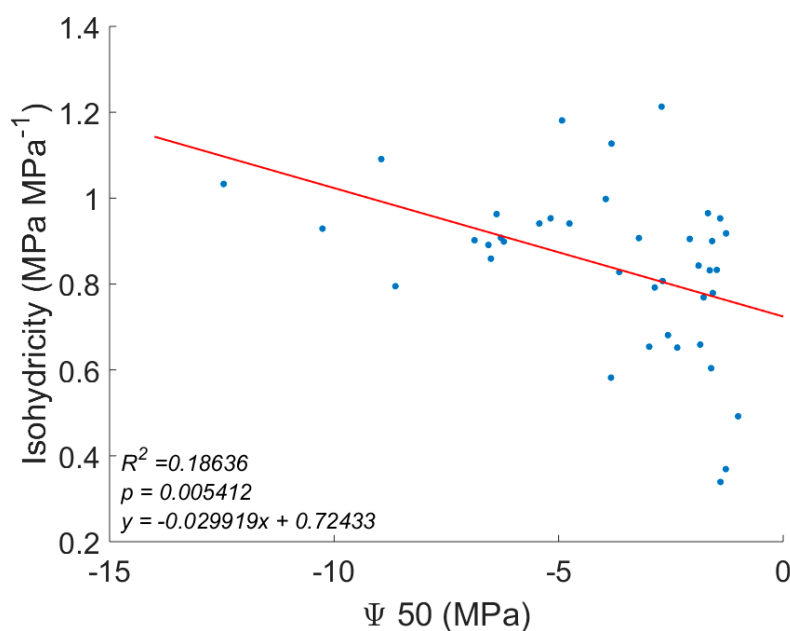


**Figure 1.** More isohydric species (isohydricity closer to 0) maintain less negative  $\Psi_{50}$  by combatting high VPD with stomatal control. ( $R^2 = 0.19$ ,  $p = 0.005$ ) Markers represent individual species ( $n = 40$ ).

A simple multiple regression model between xylem traits of  $K_{\max}$  and  $\Psi_{50}$  revealed significant covariation with rooting depth, but with a low  $R^2$  ( $R^2 = 0.1345$ ,  $p = 0.0038$ , Figure 2). The multiple linear regression stepwise model revealed further interconnectedness between variables and allowed for an analysis of the interaction terms between the traits. The stepwise model predicts isohydricity with input of leaf permanence, wood density, rooting depth, and three interaction terms, but was not statistically significant, potentially due to the small number of species for which all four traits were available ( $R^2 = 0.87$ , Prob  $< F = 0.17$ ,  $n = 10$ ). A stepwise model of drought tolerance found that drought tolerance was strongly related to wood density, isohydricity, and root depth with the inclusion of interaction terms (Adjusted  $R^2 = 0.52$ , Prob  $< F = 0.0154$ ). However, a simple multiple regression between traits at each of the leaf (isohydricity), stem (wood density), and root levels (rooting depth) was not statistically significant ( $R^2 = 0.23$ ,  $p = 0.42$ ,  $n = 23$  Figure 3). The lack of significance here may likewise be due to the limited number of species for which all three traits were available.

The boxplots and ANOVA analyses confirm known relationships of vegetation and hydraulic trends but also shed light on some additional interactions. Throughout the data, growth form appears to dictate much of the variance in the other traits. Wood density was found to increase with drought tolerance for each biome (Figure 4). Shrubs were found to have higher conduit densities but shallower

rooting depths when compared to the trees in our data set, even across all biomes for which sufficient data was available (Figures S2 and S5).

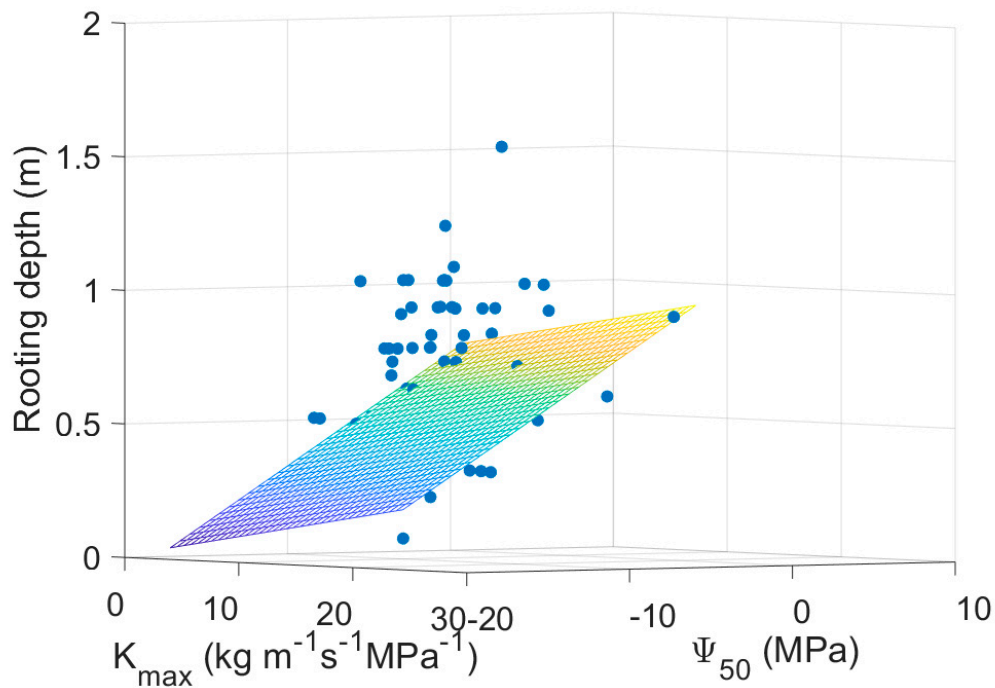


**Figure 2.** Multiple linear regression demonstrates a significant relationship between xylem traits ( $K_{\max}$  and  $\Psi_{50}$ ) and rooting depth ( $R^2 = 0.1345$ ,  $p = 0.0048$ ). Markers represent individual species ( $n = 78$ ).

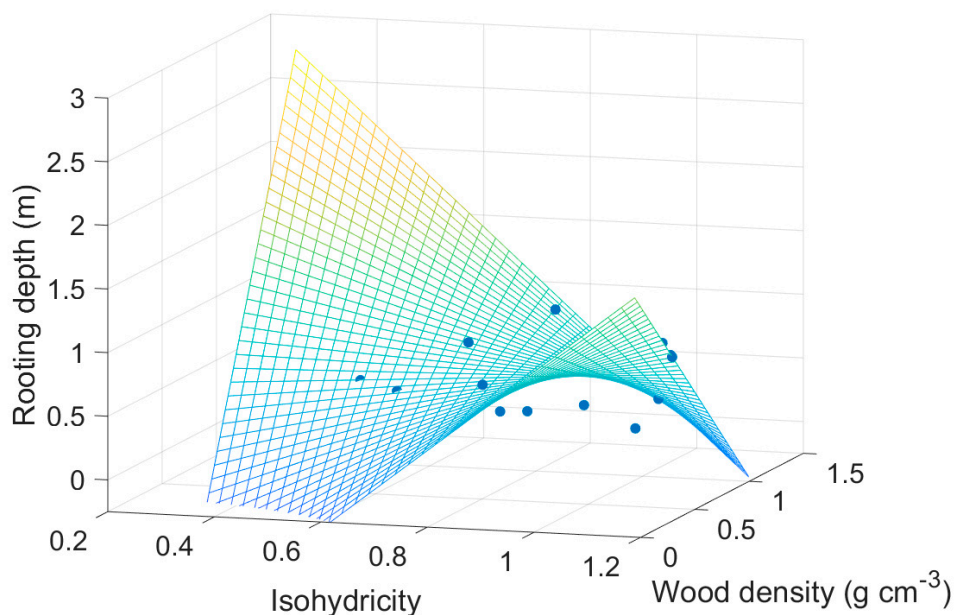


**Figure 3.** Multiple linear regression demonstrating potential trait-space described by rooting depth, isohydricity, and wood density ( $R^2 = 0.24$ ,  $p = 0.42$  \*not significant). Markers represent individual species ( $n = 23$ ).

Most trees in our study root deeper than shorter species in the same biome (Figure S5). Deciduous shrubs have a less negative  $\Psi_{50}$  than deciduous trees (Figure S8). Evergreen trees and shrubs show a wider range of  $\Psi_{50}$  than deciduous species, which could be a function of greater variability

within the subset of our compiled data (Figure S8). According to single way ANOVA, conduit density and rooting depth are also related to biome, with  $\text{Prob} > F = 0.0019$  and  $0.004$  respectively (Figures S2 and S6).

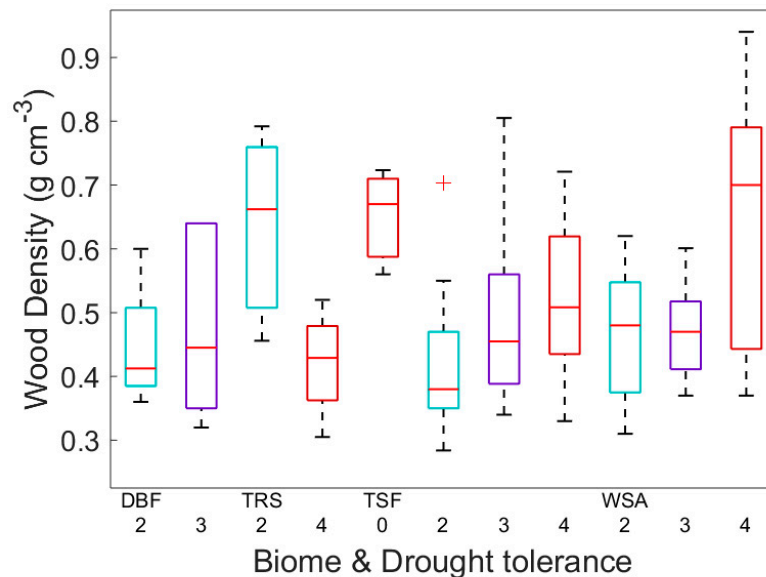


**Figure 4.** Drought tolerance generally increases with wood density. From left to right along the x-axis biomes are deciduous broadleaf forest (DBF), tropical-seasonal forest (TRS), temperate-seasonal forest (TSF), and woodland/shrubland (WSA). Missing bars are indicative of missing data for biome and drought tolerance. Drought tolerance is rated from 0 to 5 with 5 representing the most drought tolerant. Desert (DES) and tropical forests (TRO) are excluded from this figure because all species for each were listed as extremely drought tolerant (4) or extremely drought sensitive (0), respectively. Outlier values are marked with a red +.

#### 4. Discussion

Hydraulic trait correlation was demonstrated through simple and multiple linear regressions; with the relationship between rooting depth,  $K_{\max}$ , and  $\Psi_{50}$  supporting our first hypothesis that hydraulic traits will be significantly coordinated across organ levels to form hydraulic strategies (Figure 2). However, this relationship was weak ( $R^2 = 0.13$ ). While the multiple regression spanning the organ levels using rooting depth, wood density, and isohydricity (Figure 3) had a higher  $R^2$  (0.24), it was not statistically significant. This lack of significance may be due to the paucity of species for which data was available for all three of these particular traits ( $n = 23$ ).

As expected, biome and growth form are deterministic of many hydraulic traits such as wood density (Figure 4), rooting depth (Figures S5 and S6), and  $\Psi_{50}$  (Figure S8). But, these traits were also significantly related to other hydraulic traits in the absence of isolating either biome or growth form, thus supporting our second hypothesis that global correlations would exist in spite of the governing influences of vegetation form and climate. The high degree of variability within species, genus, and particularly within ecosystems and plant functional types revealed by Anderegg [65] supports this finding. Wood density was significantly related to  $a$ , the shape parameter of the xylem vulnerability curve (Figure S4) demonstrating that more dense wood tends to lose hydraulic conductivity more slowly than less dense wood. This follows logically with results in Figure 4 showing increasing drought tolerance with higher wood density. Rooting depth was well correlated with  $K_{\max}$ , and  $\Psi_{50}$  (Figure 2).  $\Psi_{50}$  was found to be related to isohydricity (Figure 1),  $K_{\max}$  (Figure S3) and rooting depth (Figure 2). The weak relationship found here between  $K_{\max}$  and  $\Psi_{50}$  is further supported by the extensive analysis performed by Gleason, et al. [17]. Most notably, in our stepwise multiple regression model of drought

tolerance, terms representing biome and growth form were found not to improve the model (Table 2). Instead, drought tolerance was best explained by wood density, rooting depth, and isohydricity (Root mean squared error (RMSE): 0.34,  $R^2 = 0.63$ , Adjusted  $R^2 = 0.52$ , Prob  $< F = 0.0154$ ).

**Table 2.** Stepwise multiple regression model for drought tolerance explained along the basis of wood density, rooting depth, and isohydricity (Overall model statistics: RMSE: 0.34,  $R^2 = 0.63$ , Adjusted  $R^2 = 0.52$ , Prob  $< F = 0.0154$ ).

	Estimate	SE	<i>t</i> Stat	<i>p</i> Value
Intercept	3.4292	0.5491	6.2455	0.0001
Wood density	0.9212	0.7688	1.1983	0.2584
Rooting depth	−1.2877	0.3644	−3.5340	0.0054
Isohydricity	0.4552	0.5172	0.8801	0.3995

Similarly to our strong support of our first hypothesis, numerous previous syntheses and database efforts have revealed coordination among vegetation hydraulic traits e.g., [17,32,37,40]. Notably, Chave, et al. [3] demonstrated relationships between wood conductivity and conduit diameter, along with relationships between wood density and both growth rate and mortality. Linkages between hydraulic traits at different organ levels (e.g., leaves and stems) have been shown for isohydricity with  $\Psi_{50}$  and  $\Psi_{88}$  for more than 100 species [58] with stronger correlations than were found in this analysis (Figure 1). Coordination between stomatal and xylem safety margins were also established by Skelton, et al. [66]. While Manzoni, et al. [16] showed covariance between xylem conductance and the driving potential gradient at maximum transpiration, suggesting strong coordination among traits at multiple organ levels throughout the vegetative hydraulic pathway. Manzoni, et al. [16] further demonstrated differences in  $K_{max}$ ,  $a$ ,  $\Psi_{50}$ , and normalized maximum transpiration rate with biome and growth form, similarly to Figure S8. A more complex mathematical framework revealed coordination between stomatal closure and  $\Psi_{50}$  to reduce the risk of embolism while maintaining transpiration [67,68]. A number of smaller-scale, biome or growth form specific studies (e.g., [12,40,69–71]) have revealed a number of more specific relationships. For instance, Blackman, et al. [71] found that among woody Australian plants, at the leaf level  $\Psi_{50}$  was significantly related to the ratio of vessel wall thickness to lumen breadth. The work of Santiago, et al. [40] revealed that for several Amazonian canopy species, xylem water-transport efficiency was connected to hydraulic capacitance, leaf turgor loss point and drought tolerance and that wood density was related to xylem cavitation curves.

The results of our global meta-analysis, when taken together with these findings, strongly indicate the presence of trait covariance and tradeoffs among plant hydraulic traits across organ levels. Within the context of a whole-plant safety-efficiency framework [16], it follows that such traits would be coordinated in a way that would maximize plants' ability to take in carbon while reducing stress on the hydraulic system. Recent work from Anderegg, et al. [72] supports the theory that stomatal control is maintained to optimize carbon uptake while avoiding hydraulic dysfunction. Our results demonstrate that in a stepwise multiple regression model, the ability of a species to tolerate drought is dependent on the combination and interactions of rooting depth, wood density, and isohydricity (Table 2). This reinforces the theory of a coordinated whole-plant hydraulic strategy governing vegetation responses to water-stress limitations, with strong implications for modeling plant hydraulic traits. For instance, the parameterization of PHMs could include traits such as rooting depth,  $K_{max}$ , and  $\Psi_{50}$  (Figure 2) along with potentially isohydricity or wood density (Figure 3) to simulate varying responses to drought. Simulations could then be benchmarked against the stepwise multiple regression model for drought tolerance (Table 2).

Recent discussion led by Hochberg, et al. [73] and Mirfenderesgi, et al. [47] emphasizes that rather than being a leaf-level trait to which it is occasionally simplified, isohydricity is representative of an emergent whole-plant hydraulic response to variable environmental conditions. Isohydricity has

been broadly used to describe stomatal or leaf-level control over water use. This terminology is rooted in the original work from Berger Landefeldt [74] observing diurnal cycles of plant water uptake. In species where stomatal conductance,  $g_s$ , is tightly regulated and therefore decoupled from the vapor pressure deficit (VPD),  $\Psi_{\text{leaf}}$  becomes decoupled from  $\Psi_{\text{soil}}$ . This behavior, referred to as isohydry, promotes greater hydraulic control in a tradeoff that may decrease growth potential in conditions where soil water availability is limited [41,75,76]. The passive, anisohydric stomatal regulation strategy, makes a prominent distinction as the opposing end-member of isohydricity, which allows stomata to remain open at the expense of very negative leaf and branch water potentials. In a large-scale synthesis study, Martinez-Vilalta, et al. [58] revealed that most species operate along a continuum between these two end members. Water potential in the roots of plants is generally coupled to soil water potential; while water potentials throughout the vegetative hydraulic pathway are strongly auto-correlated, linking stem and branch water potential gradients to leaf water potential. Finally, as stomata respond (or do not) to VPD on the basis of leaf water potential, isohydricity can be considered an integrative, whole-plant hydraulic response to the environment rather than physical trait. Therefore, it follows that, in spite of the relatively weak correlations shown in the present effort (Figures 1 and 3), that isohydricity ought to be related to other hydraulic traits as shown by Martinez-Vilalta, et al. [58]. Yet, the dependence on environmental conditions and the potential for trait variability between and within populations in diverse environmental settings along with trait plasticity specific to a site's life history may play a complicating role in the use of this trait as a proxy for others [65,77].

The repeated use of the same variables such as rooting depth, wood density,  $K_{\text{max}}$ , and  $\Psi_{50}$  in many of the statistically significant models above indicates the importance of constraining these variables for use in plant hydraulics modeling. The interrelatedness of these traits gives rise to the potential to approximate traits that are challenging to measure (i.e., rooting depth) on the basis of better studied traits such as wood density,  $K_{\text{max}}$ , or possibly isohydricity. Multidimensional trait spaces yielded by these correlations (e.g., Figures 2 and 3) permit the use of one or more trait values as a proxy for a third. Observationally constrained trait spaces can be used within dynamic global vegetation models (DGVMs) and LSM schemes to parameterize resource-use strategies of PFTs [46] or potential new classification schemes based on hydraulic strategy [18,78]. The trend for more physically based modeling is moving away from traditionally defined PFT classes and empirically-based approximations of vegetation function and towards mechanistic calculations of physiological responses through, for example, the incorporation of PHMs [44,45]. Work by Mirfenderesgi, et al. [47] demonstrated a first effort to reveal the potential of hydraulic trait spaces for the parameterization of hypothetical plant species representative of the most common hydraulic functional types and their outcomes on PHM-simulated transpiration and latent heat flux.

Standard PFT classifications made on the basis of leaf permanence and biome tend to aggregate hydraulically dissimilar species into the same category, making them less than ideal for use with new modeling schemes which employ PHMs [65]. Uncertainties in existing LSMs, and particularly water budgets, can be traced to uncertainties in distributions and characterizations of PFTs [79–81]. For instance, Poulter, et al. [82] found uncertainties as high as 30% for gross primary productivity, and 20% for evapotranspiration in the LPJmL model caused by land-cover uncertainties. A number of recent developments among DGVMs and LSMs have shifted the focus on vegetation away from PFT classifications towards this new type of more functionally based representation schemes (often referred to as 'trait-based') (e.g., [5,83–85]). Yet, in the scope of these new modeling techniques, the global availability of relevant and reliable trait observations is increasingly crucial.

## 5. Conclusions

Our results demonstrate the interconnectedness of multiple hydraulic traits, and particularly traits surrounding hydraulic conductivity and vulnerability to embolism with wood density and isohydricity. Specifically, wood density was related to the shape parameter of the xylem vulnerability curve; rooting depth was well correlated with  $K_{\text{max}}$ , and  $\Psi_{50}$ ; and  $\Psi_{50}$  was related to isohydricity,  $K_{\text{max}}$ ,

and rooting depth. Drought sensitivity was strongly (adjusted  $R^2 = 0.52$ ,  $\text{Prob} < F = 0.0154$ ) predicted by rooting depth, wood density, and isohydricity. While many traits were shown to be connected to biomes and growth form, results from simple linear and multiple regressions and stepwise multiple regressions demonstrated that traits were interrelated at a global level and not only when broken out into these categories. Notably, neither biome nor growth form significantly improved our model for drought sensitivity. These traits used for prediction span the plant hydraulic system from roots to leaves, providing an integrative description of the whole-plant hydraulic strategy. This new approach to describing hydraulic strategy through an emergent trait space is integral to providing PHMs with crucial, biologically relevant constraints for model parameterizations.

Particularly within the context of 21st century climate and land-use change, terrestrial ecosystems have a great deal of influence on the global water and carbon cycles via water storage and cycling, photosynthesis, and a variety of other feedback mechanisms with both the subsurface and the atmosphere. The complex nature of modeling the hydrosphere, which is regulated in large part by plant functions, emphasizes the need for statistical simplifications of complex ecosystem functionalities, such as water transport within biomass. Here, we put forward a first effort to establish a statistical multidimensional trait space for plant hydraulics in order to help constrain the number of trait observations and parameterizations necessary to build meaningful plant hydraulics models. Yet, we note that on the basis of relatively low  $R^2$  values and many unavailable data spanning multiple biomes (most notably boreal, taiga, and tundra) caution is imperative when attempting to extrapolate these findings to other systems. One of the major implications of this paper is the necessity for increased global coverage of plant hydraulic trait representation in broadly available databases. This will facilitate large-scale implementation and use of PHMs to improve predictions of water and carbon exchange within the terrestrial biosphere.

**Supplementary Materials:** The following are available online at <http://www.mdpi.com/1999-4907/9/8/446/s1>, Table S1: Outliers which were removed manually for extremophile species. Additional excluded outliers include conduit densities greater than 300 mm<sup>-1</sup>, root depths greater than 15 m, and precipitation values less than zero, Figure S1: Log-transformed  $K_{\max}$  increases with lower conduit density ( $R^2 = 0.27$ ,  $p = 0.0005$ ), Markers represent individual species ( $n = 41$ ), Figure S2: ANOVA analysis with conduit density per biomes desert (DES), tropical forest (TRO), tropical seasonal forest (TRS), temperate seasonal forest (TSF). Desert species have the lowest conduit density while tropical forests have the highest ( $\text{Prob} > F = 0.0019$ ), Figure S3: The positive linear relationship between log-transformed  $K_{\max}$  and the water potential at which 50% of hydraulic conductivity is lost ( $R^2 = 0.19$ ,  $p < 0.0001$ ), Markers represent individual species ( $n = 225$ ), Figure S4: Increased wood density promotes resistance to embolism which can be seen as a lower  $a$ .  $a$  is representative of the steepness of the xylem cavitation curve at  $\Psi_{50}$ . Large values of  $a$  represent faster losses in conductivity with decreasing  $\Psi$ , while smaller values represent slower declines in conductivity. ( $R^2 = 0.17$ ,  $p < 0.0001$ ) Markers represent individual species ( $n = 144$ ), Figure S5: Rooting depth differs substantially across biomes with growth form. From left to right along the x-axis biomes are desert (DES), tropical forest (TRO), tropical seasonal forest (TRS), temperate-seasonal forest (TSF), and woodland/shrubland (WSA). Trees tend to be more deeply rooted than shrubs and grasses. Missing bars are indicative of growth forms not represented within the data set for a particular biome, Figure S6: ANOVA analysis of rooting depth across desert (DES), tropical forest (TRO), tropical seasonal forest (TRS), temperate seasonal forest (TSF), and woodland/shrubland (WSA) categorized biomes (left to right) ( $\text{Prob} > F = 0.0004$ ), Figure S7: No significant relationship was found between isohydricity and rooting depth for the 22 species for which data were available ( $p = 0.57$ ), Figure S8: Evergreen trees withstand greater negative pressures than deciduous shrubs or herbs. While evergreen shrubs demonstrate a wider range of  $\Psi_{50}$  than deciduous species.

**Author Contributions:** A.R.M. and A.M.M. designed the study and wrote the body of the manuscript. A.R.M., E.M. and K.V.H. compiled the trait data from all available databases. E.M., K.V.H., L.S. and A.M.M. performed statistical analyses. All authors have edited and approved of the manuscript.

**Funding:** Funding for this work was provided by National Science Foundation Hydrological Science grant 1521238. Support for A. R. Mursinna was provided through the Burke Undergraduate Research Grant through the Jackson School of Geological Sciences and the University of Texas at Austin. Any opinions, findings, and conclusions or recommendations expressed in this material are those of the authors and do not necessarily reflect the views of the funding agencies. The study has been supported by the TRY initiative on plant traits (<http://www.try-db.org>). The TRY initiative and database is hosted, developed and maintained by J. Kattge and G. Bönsch (Max Planck Institute for Biogeochemistry, Jena, Germany). TRY is currently supported by DIVERSITAS/Future Earth and the German Centre for Integrative Biodiversity Research (iDiv) Halle-Jena-Leipzig.

**Conflicts of Interest:** The authors declare no conflict of interest.

## References

- Ackerly, D.D.; Dudley, S.A.; Sultan, S.E.; Schmitt, J.; Coleman, J.S.; Linder, C.R.; Sandquist, D.R.; Geber, M.A.; Evans, A.S.; Dawson, T.E.; et al. The evolution of plant ecophysiological traits: Recent advances and future directions new research addresses natural selection, genetic constraints, and the adaptive evolution of plant ecophysiological traits. *Bioscience* **2000**, *50*, 979–995. [[CrossRef](#)]
- Freschet, G.T.; Cornelissen, J.H.C.; van Logtestijn, R.S.P.; Aerts, R. Evidence of the ‘plant economics spectrum’ in a subarctic flora. *J. Ecol.* **2010**, *98*, 362–373. [[CrossRef](#)]
- Chave, J.; Coomes, D.; Jansen, S.; Lewis, S.L.; Swenson, N.G.; Zanne, A.E. Towards a worldwide wood economics spectrum. *Ecol. Lett.* **2009**, *12*, 351–366. [[CrossRef](#)] [[PubMed](#)]
- Reich, P.B. The world-wide ‘fast-slow’ plant economics spectrum: A traits manifesto. *J. Ecol.* **2014**, *102*, 275–301. [[CrossRef](#)]
- Sakschewski, B.; von Bloh, W.; Boit, A.; Rammig, A.; Kattge, J.; Poorter, L.; Penuelas, J.; Thonicke, K. Leaf and stem economics spectra drive diversity of functional plant traits in a dynamic global vegetation model. *Glob. Chang. Biol.* **2015**, *21*, 2711–2725. [[CrossRef](#)] [[PubMed](#)]
- Wright, I.J.; Reich, P.B.; Westoby, M.; Ackerly, D.D.; Baruch, Z.; Bongers, F.; Cavender-Bares, J.; Chapin, T.; Cornelissen, J.H.C.; Diemer, M.; et al. The worldwide leaf economics spectrum. *Nature* **2004**, *428*, 821–827. [[CrossRef](#)] [[PubMed](#)]
- Reich, P.B.; Wright, I.J.; Lusk, C.H. Predicting leaf physiology from simple plant and climate attributes: A global glopnet analysis. *Ecol. Appl.* **2007**, *17*, 1982–1988. [[CrossRef](#)] [[PubMed](#)]
- Wright, I.J.; Reich, P.B.; Cornelissen, J.H.C.; Falster, D.S.; Garnier, E.; Hikosaka, K.; Lamont, B.B.; Lee, W.; Oleksyn, J.; Osada, N.; et al. Assessing the generality of global leaf trait relationships. *New Phytol.* **2005**, *166*, 485–496. [[CrossRef](#)] [[PubMed](#)]
- Messier, J.; McGill, B.J.; Lechowicz, M.J. How do traits vary across ecological scales? A case for trait-based ecology. *Ecol. Lett.* **2010**, *13*, 838–848. [[CrossRef](#)] [[PubMed](#)]
- Zhu, S.-D.; Chen, Y.-J.; Ye, Q.; He, P.-C.; Liu, H.P.; Li, R.-H.; Fu, P.-L.; Jiang, G.-F.; Cao, K.-F. Leaf turgor loss point is correlated with drought tolerance and leaf carbon economics traits. *Tree Physiol.* **2018**, *38*, 658–663. [[CrossRef](#)] [[PubMed](#)]
- Sack, L.; Holbrook, N.M. Leaf hydraulics. In *Annual Review Plant biology*; Annual Reviews: Palo Alto, CA, USA, 2006; Volume 57, pp. 361–381.
- Fu, P.-L.; Jiang, Y.-J.; Wang, A.-Y.; Brodribb, T.J.; Zhang, J.-L.; Zhu, S.-D.; Cao, K.-F. Stem hydraulic traits and leaf water-stress tolerance are co-ordinated with the leaf phenology of angiosperm trees in an Asian tropical dry karst forest. *Ann. Bot.* **2012**, *110*, 189–199. [[CrossRef](#)] [[PubMed](#)]
- Nardini, A.; Peda, G.; La Rocca, N. Trade-offs between leaf hydraulic capacity and drought vulnerability: Morpho-anatomical bases, carbon costs and ecological consequences. *New Phytol.* **2012**, *196*, 788–798. [[CrossRef](#)] [[PubMed](#)]
- Jin, Y.; Wang, C.K.; Zhou, Z.H.; Li, Z.M. Co-ordinated performance of leaf hydraulics and economics in 10 Chinese temperate tree species. *Funct. Plant Biol.* **2016**, *43*, 1082–1090. [[CrossRef](#)]
- Tyree, M.T.; Zimmermann, M.H. Xylem structure and the ascent of sap. In *Xylem Structure and the Ascent of Sap*; Springer: New York, NY, USA, 2002.
- Manzoni, S.; Vico, G.; Katul, G.G.; Palmroth, S.; Jackson, R.B.; Porporato, A. Hydraulic limits on maximum plant transpiration and the emergence of the safety-efficiency trade-off. *New Phytol.* **2013**, *198*, 169–178. [[CrossRef](#)] [[PubMed](#)]
- Gleason, S.M.; Westoby, M.; Jansen, S.; Choat, B.; Hacke, U.G.; Pratt, R.B.; Bhaskar, R.; Brodribb, T.J.; Bucci, S.J.; Cao, K.F.; et al. Weak tradeoff between xylem safety and xylem-specific hydraulic efficiency across the world’s woody plant species. *New Phytol.* **2016**, *209*, 123–136. [[CrossRef](#)] [[PubMed](#)]
- Matheny, A.M.; Mirfenderesgi, G.; Bohrer, G. Trait-based representation of hydrological functional properties of plants in weather and ecosystem models. *Plant Divers.* **2017**, *39*, 1–12. [[CrossRef](#)]
- Griffin-Nolan, R.J.; Bushey, J.A.; Carroll, C.J.W.; Challis, A.; Chieppa, J.; Garbowski, M.; Hoffman, A.M.; Post, A.K.; Slette, I.J.; Spitzer, D.; et al. Trait selection and community weighting are key to understanding ecosystem responses to changing precipitation regimes. *Funct. Ecol.* **2018**. [[CrossRef](#)]

20. Allen, C.D.; Macalady, A.K.; Chenchouni, H.; Bachelet, D.; McDowell, N.; Venetier, M.; Kitzberger, T.; Rigling, A.; Breshears, D.D.; Hogg, E.H.; et al. A global overview of drought and heat-induced tree mortality reveals emerging climate change risks for forests. *For. Ecol. Manag.* **2010**, *259*, 660–684. [[CrossRef](#)]
21. Anderegg, W.R.L.; Berry, J.A.; Smith, D.D.; Sperry, J.S.; Anderegg, L.D.L.; Field, C.B. The roles of hydraulic and carbon stress in a widespread climate-induced forest die-off. *Proc. Natl. Acad. Sci. USA* **2012**, *109*, 233–237. [[CrossRef](#)] [[PubMed](#)]
22. Fu, R.; Yin, L.; Li, W.H.; Arias, P.A.; Dickinson, R.E.; Huang, L.; Chakraborty, S.; Fernandes, K.; Liebmann, B.; Fisher, R.; et al. Increased dry-season length over southern amazonia in recent decades and its implication for future climate projection. *Proc. Natl. Acad. Sci. USA* **2013**, *110*, 18110–18115. [[CrossRef](#)] [[PubMed](#)]
23. Bonal, D.; Burban, B.; Stahl, C.; Wagner, F.; Herault, B. The response of tropical rainforests to drought—lessons from recent research and future prospects. *Ann. For. Sci.* **2016**, *73*, 27–44. [[CrossRef](#)] [[PubMed](#)]
24. Phillips, O.L.; van der Heijden, G.; Lewis, S.L.; Lopez-Gonzalez, G.; Aragao, L.; Lloyd, J.; Malhi, Y.; Monteagudo, A.; Almeida, S.; Davila, E.A.; et al. Drought-mortality relationships for tropical forests. *New Phytol.* **2010**, *187*, 631–646. [[CrossRef](#)] [[PubMed](#)]
25. McDowell, N.; Pockman, W.T.; Allen, C.D.; Breshears, D.D.; Cobb, N.; Kolb, T.; Plaut, J.; Sperry, J.S.; West, A.; Williams, D.G.; et al. Mechanisms of plant survival and mortality during drought: Why do some plants survive while others succumb to drought? *New Phytol.* **2008**, *178*, 719–739. [[CrossRef](#)] [[PubMed](#)]
26. McDowell, N.G.; Fisher, R.A.; Xu, C.G.; Domec, J.C.; Holttta, T.; Mackay, D.S.; Sperry, J.S.; Boutz, A.; Dickman, L.; Gehres, N.; et al. Evaluating theories of drought-induced vegetation mortality using a multimodel-experiment framework. *New Phytol.* **2013**, *200*, 304–321. [[CrossRef](#)] [[PubMed](#)]
27. Matheny, A.M.; Bohrer, G.; Vogel, C.S.; Morin, T.H.; He, L.; Frasson, R.P.M.; Mirfenderesgi, G.; Schäfer, K.V.R.; Gough, C.M.; Ivanov, V.Y.; et al. Species-specific transpiration responses to intermediate disturbance in a northern hardwood forest. *J. Geophys. Res.* **2014**, *119*, 2292–2311. [[CrossRef](#)]
28. Ford, C.R.; Hubbard, R.M.; Kloeppel, B.D.; Vose, J.M. A comparison of sap flux-based evapotranspiration estimates with catchment-scale water balance. *Agric. For. Meteorol.* **2007**, *145*, 176–185. [[CrossRef](#)]
29. Pappas, C.; Matheny, A.M.; Baltzer, J.L.; Barr, A.G.; Black, T.A.; Bohrer, G.; Detto, M.; Maillet, J.; Roy, A.; Sontentag, O.; et al. Boreal tree hydrodynamics: Asynchronous, diverging, yet complementary. *Tree Physiol.* **2018**, *38*, 953–964. [[CrossRef](#)] [[PubMed](#)]
30. McCulloh, K.A.; Johnson, D.M.; Meinzer, F.C.; Voelker, S.L.; Lachenbruch, B.; Domec, J.-C. Hydraulic architecture of two species differing in wood density: Opposing strategies in co-occurring tropical pioneer trees. *Plant Cell Environ.* **2012**, *35*, 116–125. [[CrossRef](#)] [[PubMed](#)]
31. Breshears, D.D.; Myers, O.B.; Johnson, S.R.; Meyer, C.W.; Martens, S.N. Differential use of spatially heterogeneous soil moisture by two semiarid woody species: *Pinus edulis* and *Juniperus monosperma*. *J. Ecol.* **1997**, *85*, 289–299. [[CrossRef](#)]
32. Anderegg, W.R.L.; Klein, T.; Bartlett, M.; Sack, L.; Pellegrini, A.F.A.; Choat, B.; Jansen, S. Meta-analysis reveals that hydraulic traits explain cross-species patterns of drought-induced tree mortality across the globe. *Proc. Natl. Acad. Sci. USA* **2016**, *113*, 5024–5029. [[CrossRef](#)] [[PubMed](#)]
33. Bartlett, M.K.; Klein, T.; Jansen, S.; Choat, B.; Sack, L. The correlations and sequence of plant stomatal, hydraulic, and wilting responses to drought. *Proc. Natl. Acad. Sci. USA* **2016**, *113*, 13098–13103. [[CrossRef](#)] [[PubMed](#)]
34. Bartlett, M.K.; Scoffoni, C.; Sack, L. The determinants of leaf turgor loss point and prediction of drought tolerance of species and biomes: A global meta-analysis. *Ecol. Lett.* **2012**, *15*, 393–405. [[CrossRef](#)] [[PubMed](#)]
35. Bartlett, M.K.; Zhang, Y.; Kreidler, N.; Sun, S.W.; Ardy, R.; Cao, K.F.; Sack, L. Global analysis of plasticity in turgor loss point, a key drought tolerance trait. *Ecol. Lett.* **2014**, *17*, 1580–1590. [[CrossRef](#)] [[PubMed](#)]
36. Maréchaux, I.; Bartlett, M.K.; Gaucher, P.; Sack, L.; Chave, J. Causes of variation in leaf-level drought tolerance within an amazonian forest. *J. Plant Hydraul.* **2016**, *3*, e004. [[CrossRef](#)]
37. Choat, B.; Jansen, S.; Brodribb, T.J.; Cochard, H.; Delzon, S.; Bhaskar, R.; Bucci, S.J.; Feild, T.S.; Gleason, S.M.; Hacke, U.G.; et al. Global convergence in the vulnerability of forests to drought. *Nature* **2012**, *491*, 752–756. [[CrossRef](#)] [[PubMed](#)]
38. Hoffmann, W.A.; Marchin, R.M.; Abit, P.; Lau, O.L. Hydraulic failure and tree dieback are associated with high wood density in a temperate forest under extreme drought. *Glob. Chang. Biol.* **2011**, *17*, 2731–2742. [[CrossRef](#)]

39. Meinzer, F.C.; Woodruff, D.R.; Marias, D.E.; Smith, D.D.; McCulloh, K.A.; Howard, A.R.; Magedman, A.L. Mapping ‘hydroscares’ along the iso- to anisohydric continuum of stomatal regulation of plant water status. *Ecol. Lett.* **2016**, *19*, 1343–1352. [[CrossRef](#)] [[PubMed](#)]
40. Santiago, L.S.; De Guzman, M.E.; Baraloto, C.; Vogenberg, J.; Brodie, M.; Herault, B.; Fortunel, C.; Bonal, D. Coordination and trade-offs among hydraulic safety, efficiency, and drought avoidance traits in amazonian rainforest canopy tree species. *New Phytol.* **2018**, *218*, 1015–1024. [[CrossRef](#)] [[PubMed](#)]
41. Matheny, A.M.; Fiorella, R.P.; Bohrer, G.; Poulsen, C.J.; Morin, T.H.; Wunderlich, A.; Vogel, C.S.; Curtis, P.S. Contrasting strategies of hydraulic control in two codominant temperate tree species. *Ecohydrology* **2017**, *10*, e1815. [[CrossRef](#)]
42. Mirfenderesgi, G.; Bohrer, G.; Matheny, A.M.; Fatichi, S.; Frasson, R.P.M.; Schäfer, K.V.R. Tree level hydrodynamic approach for resolving aboveground water storage and stomatal conductance and modeling the effects of tree hydraulic strategy. *J. Geophys. Res.* **2016**, *121*, 1792–1813. [[CrossRef](#)]
43. Fatichi, S.; Pappas, C.; Ivanov, V.Y. Modeling plant–water interactions: An ecohydrological overview from the cell to the global scale. *Wiley Interdiscip. Rev. Water* **2016**, *3*, 327–368. [[CrossRef](#)]
44. Christoffersen, B.O.; Gloor, M.; Fauset, S.; Fyllas, N.M.; Galbraith, D.R.; Baker, T.R.; Kruijt, B.; Rowland, L.; Fisher, R.A.; Binks, O.J.; et al. Linking hydraulic traits to tropical forest function in a size-structured and trait-driven model (tfs v.1-hydro). *Geosci. Model Dev.* **2016**, *9*, 4227–4255. [[CrossRef](#)]
45. Xu, X.; Medvigy, D.; Powers, J.S.; Becknell, J.M.; Guan, K. Diversity in plant hydraulic traits explains seasonal and inter-annual variations of vegetation dynamics in seasonally dry tropical forests. *New Phytol.* **2016**, *121*, 80–95. [[CrossRef](#)] [[PubMed](#)]
46. Fisher, R.A.; Koven, C.D.; Anderegg, W.R.L.; Christoffersen, B.O.; Dietze, M.C.; Farrior, C.E.; Holm, J.A.; Hurr, G.C.; Knox, R.G.; Lawrence, P.J.; et al. Vegetation demographics in earth system models: A review of progress and priorities. *Glob. Chang. Biol.* **2018**, *24*, 35–54. [[CrossRef](#)] [[PubMed](#)]
47. Mirfenderesgi, G.; Matheny, A.M.; Bohrer, G. Hydrodynamics trait coordination and cost-benefit trade-offs throughout the isohydric-anisohydric continuum in trees. *Ecohydrology* **2017**, accepted.
48. Lawrence, D.; Fisher, R.; Koven, C.; Oleson, K.W.; Vertenstein, M.; Andre, B.; Bonan, G.; Ghimire, B.; van Kampenhou, L.; Kennedy, D.; et al. *Technical Description of Version 5.0 of the Community Land Model (Cm)*; Research, N.C.f.A., Ed.; National Center for Atmospheric Research: Boulder, CO, USA, 2018.
49. Gentine, P.; Guérin, M.; Uriarte, M.; McDowell, N.G.; Pockman, W.T. An allometry-based model of the survival strategies of hydraulic failure and carbon starvation. *Ecohydrology* **2015**, *9*, 529–546. [[CrossRef](#)]
50. Roman, D.T.; Novick, K.A.; Brzostek, E.R.; Dragoni, D.; Rahman, F.; Phillips, R.P. The role of isohydric and anisohydric species in determining ecosystem-scale response to severe drought. *Oecologia* **2015**, *179*, 641–654. [[CrossRef](#)] [[PubMed](#)]
51. Sperry, J.S.; Adler, F.R.; Campbell, G.S.; Comstock, J.P. Limitation of plant water use by rhizosphere and xylem conductance: Results from a model. *Plant Cell Environ.* **1998**, *21*, 347–359. [[CrossRef](#)]
52. Matheny, A.M.; Garrity, S.R.; Bohrer, G. The calibration and use of capacitance sensors to monitor stem water content in trees. *J. Vis. Exp.* **2017**, e57062. [[CrossRef](#)]
53. Huang, C.-W.; Domec, J.-C.; Ward, E.J.; Duman, T.; Manoli, G.; Parolari, A.J.; Katul, G.G. The effect of plant water storage on water fluxes within the coupled soil–plant system. *New Phytol.* **2017**, *213*, 1093–1106. [[CrossRef](#)] [[PubMed](#)]
54. Fatichi, S.; Ivanov, V.Y. Interannual variability of evapotranspiration and vegetation productivity. *Water Resour. Res.* **2014**, *50*, 3275–3294. [[CrossRef](#)]
55. Sperry, J.S.; Venturas, M.D.; Anderegg, W.R.L.; Mencuccini, M.; Mackay, D.S.; Wang, Y.P.; Love, D.M. Predicting stomatal responses to the environment from the optimization of photosynthetic gain and hydraulic cost. *Plant Cell Environ.* **2017**, *40*, 816–830. [[CrossRef](#)] [[PubMed](#)]
56. Wolf, A.; Anderegg, W.R.; Pacala, S.W. Optimal stomatal behavior with competition for water and risk of hydraulic impairment. *Proc. Natl Acad. Sci.* **2016**, *113*, E7222–E7230. [[CrossRef](#)] [[PubMed](#)]
57. Kattge, J.; Diaz, S.; Lavorel, S.; Prentice, C.; Leadley, P.; Bonisch, G.; Garnier, E.; Westoby, M.; Reich, P.B.; Wright, I.J.; et al. Try—A global database of plant traits. *Glob. Change Biol.* **2011**, *17*, 2905–2935. [[CrossRef](#)]
58. Martinez-Vilalta, J.; Poyatos, R.; Aguade, D.; Retana, J.; Mencuccini, M. A new look at water transport regulation in plants. *New Phytol.* **2014**, *204*, 105–115. [[CrossRef](#)] [[PubMed](#)]

59. Medlyn, B.; Badeck, F.W.; De Pury, D.; Barton, C.; Broadmeadow, M.; Ceulemans, R.; De Angelis, P.; Forstreuter, M.; Jach, M.; Kellomäki, S. Effects of elevated [CO<sub>2</sub>] on photosynthesis in european forest species: A meta-analysis of model parameters. *Plant Cell Environ.* **1999**, *22*, 1475–1495. [[CrossRef](#)]
60. Preston, K.A.; Cornwell, W.K.; DeNoyer, J.L. Wood density and vessel traits as distinct correlates of ecological strategy in 51 California coast range angiosperms. *New Phytol.* **2006**, *170*, 807–818. [[CrossRef](#)] [[PubMed](#)]
61. Green, W.A. *USDA Plants Compilation*; Version 1; 09-02; 2009. Available online: <https://plants.sc.egov.usda.gov/java/> (accessed on 25 July 2018).
62. Fitter, A.H.; Peat, H.J. The ecological flora database. *J. Ecol.* **1994**, *82*, 415–425. [[CrossRef](#)]
63. Diaz, S.; Hodgson, J.; Thompson, K.; Cabido, M.; Cornelissen, J.H.C.; Jalili, A.; Montserrat-Marti, G.; Grime, J.; Zarrinkamar, F.; Asri, Y. The plant traits that drive ecosystems: Evidence from three continents. *J. Veg. Sci.* **2004**, *15*, 295–304. [[CrossRef](#)]
64. Zanne, A.E.; Westoby, M.; Falster, D.S.; Ackerly, D.D.; Loarie, S.R.; Arnold, S.E.; Coomes, D.A. Angiosperm wood structure: Global patterns in vessel anatomy and their relation to wood density and potential conductivity. *Am. J. Bot.* **2010**, *97*, 207–215. [[CrossRef](#)] [[PubMed](#)]
65. Anderegg, W.R.L. Spatial and temporal variation in plant hydraulic traits and their relevance for climate change impacts on vegetation. *New Phytol.* **2015**, *205*, 1008–1014. [[CrossRef](#)] [[PubMed](#)]
66. Skelton, R.P.; West, A.G.; Dawson, T.E. Predicting plant vulnerability to drought in biodiverse regions using functional traits. *Proc. Natl. Acad. Sci. USA* **2015**, *112*, 5744–5749. [[CrossRef](#)] [[PubMed](#)]
67. Manzoni, S.; Katul, G.; Porporato, A. A dynamical system perspective on plant hydraulic failure. *Water Resour. Res.* **2014**, *50*, 5170–5183. [[CrossRef](#)]
68. Manzoni, S.; Vico, G.; Katul, G.; Palmroth, S.; Porporato, A. Optimal plant water-use strategies under stochastic rainfall. *Water Resour. Res.* **2014**, *50*, 5379–5394. [[CrossRef](#)]
69. Santiago, L.S.; Goldstein, G.; Meinzer, F.C.; Fisher, J.B.; Machado, K.; Woodruff, D.; Jones, T. Leaf photosynthetic traits scale with hydraulic conductivity and wood density in panamanian forest canopy trees. *Oecologia* **2004**, *140*, 543–550. [[CrossRef](#)] [[PubMed](#)]
70. Zhou, S.X.; Medlyn, B.; Sabate, S.; Sperlich, D.; Prentice, I.C. Short-term water stress impacts on stomatal, mesophyll and biochemical limitations to photosynthesis differ consistently among tree species from contrasting climates. *Tree Physiol.* **2014**, *34*, 1035–1046. [[CrossRef](#)] [[PubMed](#)]
71. Blackman, C.J.; Gleason, S.M.; Cook, A.M.; Chang, Y.; Laws, C.A.; Westoby, M. The links between leaf hydraulic vulnerability to drought and key aspects of leaf venation and xylem anatomy among 26 australian woody angiosperms from contrasting climates. *Ann. Bot.* **2018**, *122*, 59–67. [[CrossRef](#)] [[PubMed](#)]
72. Anderegg, W.R.L.; Wolf, A.; Arango-Velez, A.; Choat, B.; Chmura, D.J.; Jansen, S.; Kolb, T.; Li, S.; Meinzer, F.C.; Pita, P.; et al. Woody plants optimise stomatal behaviour relative to hydraulic risk. *Ecol. Lett.* **2018**, *21*, 968–977. [[CrossRef](#)] [[PubMed](#)]
73. Hochberg, U.; Rockwell, F.E.; Holbrook, N.M.; Cochard, H. Iso/anisohydry: A plant–environment interaction rather than a simple hydraulic trait. *Trends Plant Sci.* **2018**, *23*, 112–120. [[CrossRef](#)] [[PubMed](#)]
74. Berger Landefeldt, U. Das wasserhaushalt der alpenflanzen. *Bibl. Bot* **1936**, *115*, 81.
75. Voelker, S.L.; DeRose, R.J.; Bekker, M.F.; Sriladda, C.; Leksungnoen, N.; Kjelgren, R.K. Anisohydric water use behavior links growing season evaporative demand to ring-width increment in conifers from summer-dry environments. *Trees* **2018**, *32*, 735–749. [[CrossRef](#)]
76. Konings, A.G.; Williams, A.P.; Gentine, P. Sensitivity of grassland productivity to aridity controlled by stomatal and xylem regulation. *Nat. Geosci.* **2017**, *10*, 284. [[CrossRef](#)]
77. Anderegg, L.D.L.; Berner, L.T.; Badgley, G.; Sethi, M.L.; Law, B.E.; HilleRisLambers, J. Within-species patterns challenge our understanding of the leaf economics spectrum. *Ecol. Lett.* **2018**, *21*, 734–744. [[CrossRef](#)] [[PubMed](#)]
78. Yang, Y.Z.; Zhu, Q.A.; Peng, C.H.; Wang, H.; Chen, H. From plant functional types to plant functional traits: A new paradigm in modelling global vegetation dynamics. *Prog. Phys. Geogr.* **2015**, *39*, 514–535. [[CrossRef](#)]
79. Matheny, A.M.; Bohrer, G.; Stoy, P.C.; Baker, I.; Black, A.T.; Desai, A.R.; Dietze, M.; Gough, C.M.; Ivanov, V.Y.; Jassal, R.; et al. Characterizing the diurnal patterns of errors in the prediction of evapotranspiration by several land-surface models: An nacp analysis. *J. Geophys. Res.* **2014**, *119*, 1458–1473. [[CrossRef](#)]
80. Sitch, S.; Smith, B.; Prentice, I.C.; Arneth, A.; Bondeau, A.; Cramer, W.; Kaplan, J.O.; Levis, S.; Lucht, W.; Sykes, M.T.; et al. Evaluation of ecosystem dynamics, plant geography and terrestrial carbon cycling in the lpj dynamic global vegetation model. *Glob. Change Biol.* **2003**, *9*, 161–185. [[CrossRef](#)]

81. Sun, W.X.; Liang, S.L.; Xu, G.; Fang, H.L.; Dickinson, R. Mapping plant functional types from modis data using multisource evidential reasoning. *Remote Sens. Environ.* **2008**, *112*, 1010–1024. [[CrossRef](#)]
82. Poulter, B.; Ciais, P.; Hodson, E.; Lischke, H.; Maignan, F.; Plummer, S.; Zimmermann, N.E. Plant functional type mapping for earth system models. *Geosci. Model Dev.* **2011**, *4*, 993–1010. [[CrossRef](#)]
83. Pappas, C.; Fatichi, S.; Burlando, P. Modeling terrestrial carbon and water dynamics across climatic gradients: Does plant trait diversity matter? *New Phytol.* **2016**, *209*, 137–151. [[CrossRef](#)] [[PubMed](#)]
84. Musavi, T.; Mahecha, M.D.; Migliavacca, M.; Reichstein, M.; van de Weg, M.J.; van Bodegom, P.M.; Bahn, M.; Wirth, C.; Reich, P.B.; Schrod, F.; et al. The imprint of plants on ecosystem functioning: A data-driven approach. *Int. J. Appl. Earth Obs. Geoinf.* **2015**, *43*, 119–131. [[CrossRef](#)]
85. Reichstein, M.; Bahn, M.; Mahecha, M.D.; Kattge, J.; Baldocchi, D.D. Linking plant and ecosystem functional biogeography. *Proc. Natl Acad. Sci. USA* **2014**, *111*, 13697–13702. [[CrossRef](#)] [[PubMed](#)]



© 2018 by the authors. Licensee MDPI, Basel, Switzerland. This article is an open access article distributed under the terms and conditions of the Creative Commons Attribution (CC BY) license (<http://creativecommons.org/licenses/by/4.0/>).